

# Design of a Cost Effective Thrust Stand for Introducing Thrust and Impulse

Ethan Hopping<sup>1</sup>

*The University of Alabama in Huntsville, Huntsville, AL, 35899*

Markus Murdy<sup>2</sup>

*The University of Alabama in Huntsville, Huntsville, AL, 35899*

Nathaniel Stepp<sup>2</sup>

*The University of Alabama in Huntsville, Huntsville, AL, 35899*

**A thrust stand was designed and manufactured to demonstrate principles of thrust and impulse to students in an introductory aerospace engineering course at the University of Alabama in Huntsville. In this course, students are introduced to basic principles of flight by designing rubber band powered airplanes with the goal of maximizing mass of a U.S. penny payload per unit flight distance. One of the factors limiting student analysis was a lack of information about the rubber band and propeller thrust characteristics. The thrust stand allows student groups to measure the thrust characteristics of their specific rubber band and propeller configuration. The thrust stand was constructed using 8020 T-slot framing and had a total cost of less than 300 dollars. A data acquisition system was designed around the Arduino UNO microcontroller and an instrumentation amplifier; force was read through a full bridge strain gauge rated for a max loading of 0.3kg. MATLAB was used to develop a graphical user interface for data collection and analysis. Resultant thrust stand operation and performance data are presented.**

## Nomenclature

<i>ADC</i>	= analogue to digital converter
<i>DAQ</i>	= data acquisition system
<i>FDM</i>	= fused deposition modelling
<i>FFT</i>	= fast fourier transform
<i>GUI</i>	= graphical user interface
<i>ICSP</i>	= in-circuit system programmer
<i>IDE</i>	= integrated development environment
<i>LPF</i>	= low pass filter
<i>LSB</i>	= least significant bit (un-calibrated ADC readings)
<i>UAV</i>	= unmanned aerial vehicle
<i>USART</i>	= universal synchronous and asynchronous serial receiver and transmitter

## I. Introduction

Thrust and impulse are critical parameters to consider for analyses of the performance of any propulsion system. Since propulsion systems are a basic requirement for heavier than air flight, it is important that aerospace students possess a basic understanding of the significance of thrust and impulse with regard to propulsion systems and powered flight. Hands-on demonstrations of physical concepts are often the most effective method for providing students with an intuitive understanding of a concept; impulse and thrust are concepts that aerospace students should understand intuitively. In the interest of providing students with a hands on demonstration of thrust and impulse, a thrust stand and supporting lab material were developed for use in an introductory aerospace engineering course at the University of Alabama in Huntsville.

---

<sup>1</sup> Undergraduate, Mechanical and Aerospace Engineering Department, eph0003@uah.edu, AIAA Student Member

<sup>2</sup> Undergraduate, Mechanical and Aerospace Engineering Department, mrm0019@uah.edu, AIAA Student Member

<sup>3</sup> Undergraduate, Mechanical and Aerospace Engineering Department, nas0009@uah.edu, AIAA Student Member

A major component of the undergraduate aerospace engineering course is a project where student teams design and construct a rubber band powered airplane from recyclable material. In construction of the aircraft, teams are encouraged to apply aerodynamic analysis to design their planes to maximize mass of a U.S. penny payload per unit flight distance. The scope of this analysis has been limited in the past because students lack performance information on the thrust characteristics of their specific propeller and rubber band configurations. The thrust stand will mitigate this limitation by providing students with a tool for measuring the performance of their specific propeller configuration and using the data to optimize aircraft performance.

The thrust stand was designed and constructed with the precision required to measure the small forces generated by a rubber band airplane. 8020 t-slot framing was used for construction of the thrust stand to ensure durability and provide a flexible design. Rapid prototyped components fabricated using FDM were also used extensively in the frame design. Thrust measurements were made using a small full bridge load cell rated for a maximum force of 0.3kg.

An additional requirement was that the thrust stand be simple to operate for student use. A GUI was developed in MATLAB for communicating with the thrust stand DAQ and plotting force measurements for analysis. The GUI is critical because it allows students to quickly obtain the measurements of interest and reset the thrust stand for repeated tests. In addition, a noise reduction tool was included in the GUI using the MATLAB FFT function for removing interference from rubber band and propeller bounce in measurement data.

Discussions of the mechanical, electrical, and software design of the thrust stand are provided in subsequent sections. These sections are followed by an analysis of the thrust stand performance through several test runs and a discussion of additional future applications for the thrust stand.

## II. Mechanical Design

The design of a thrust stand is not an original concept. Many thrust stand designs exist in the world, and most function within the design objectives of their builder. Likewise, this thrust stand design project had its own design objectives. While measuring small impulses, it also needed to be able to function in a teaching laboratory environment. This environment dictated that the thrust stand physical structure be low maintenance and easy to work with. With these objectives in mind, the team selected a hanging pendulum style for the base conceptual design. Aluminum extrusion bars, sleek and easy to clean, were used for the frame. They also provide an easy interface for future upgrades. The connectors were 3D printed variants of commercial designs, both to reduce out of pocket cost and potentially stimulate interest from the end users in this exciting new technology. These materials convey a professional appearance and are easy to maintain. The thrust stand created was an easy to use, visually appealing, addition to the undergraduate aeronautical curriculum.

### A. General Mechanical Concept

The concept for the thrust stand's hanging pendulum design was derived from NASA Marshall's Electric Space Propulsion Vacuum Test Stand. This test stand measures the thrust from different electric propulsion concepts, usually only a few Newtons, in a vacuum chamber. The NASA design needed to be low cost and effectively maintenance free for vacuum chamber use. These traits were also highly desirable qualities for this thrust stand.

The hanging pendulum concept places the thrust source on an arm, suspended below a load cell. This design is a dynamically stable configuration in earth's gravitational field, as opposed to placing the thrust source above the load cell. For this thrust stand the load cell is not placed under any sustained loading, except during data collection, and the thrust source is easily accessible. The hanging pendulum concept also provides a simple to integrate mechanical amplification of force, accomplished by adjusting the lengths of the pendulum arms.

The basic design consists of the thrust source (in this case a rubber band connected to a propeller) hanging on a pendulum. An arm of the pendulum sticks out at the base and pushes on a load cell. This C shape configuration is used to transfer horizontal motion from the propeller, to vertical motion at the load cell. The

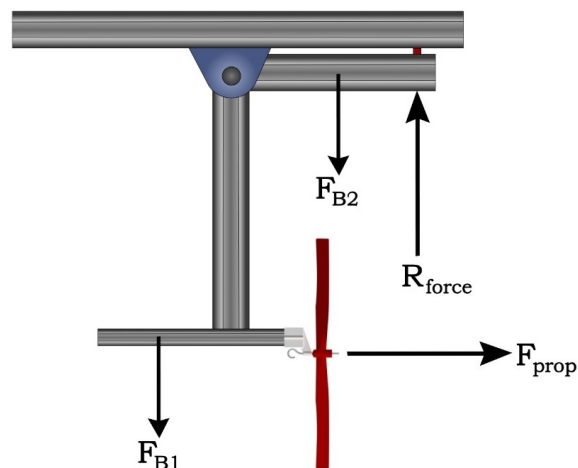


Figure 1 Thrust Stand Static Diagram

entire assembly is hung from an overhead bar. The system does not require additional support to keep the pendulum in a position different than its lowest gravitational potential energy state.

A static free-body diagram of the hanging pendulum is depicted in Figure 1.  $F_{prop}$  represents expected force created by the propeller measured in Newtons,  $R_{force}$  represents the expected reaction force of the lever arm measured in Newtons, and FB1 and FB2 represent the forces created by masses of the extensions of the lever arms represented in Newtons.

Assuming a perfectly rigid structure and the system is in static equilibrium, the following static equation (Eq. 1) can be derived to describe the force behavior of the pendulum.

$$\begin{aligned} \sum M_b = 0 &= F_{Prop}D_{FPB} + F_{B2}D_{FB2B} - F_{B1}D_{FB1B} - R_yD_{RyB} \\ \Rightarrow F_p &= \frac{-F_{B2}D_{FB2B} + F_{B1}D_{FB1B} + R_yD_{RyB}}{D_{FPB}} \end{aligned} \quad (1)$$

Eq. 1 was used to choose beam lengths for the thrust stand moment arm. The equation is under constrained with four unknowns: the lengths of the three beams and the position of the propeller-mount beam center of gravity relative to the moment point. Beam lengths were chosen by solving Eq. 1 to satisfy two specific conditions. In static equilibrium with no thrust from the rubber band propulsion system, it was desired that the static load on the load cell be as small as possible. Therefore, beam lengths were chosen such that the sum of moments around the moment point was zero under the static condition. The moment arm also needed to magnify the propeller force by a suitable factor to make the thrust measurable by the load cell. A maximum thrust of 1N was estimated for the rubber band propulsion system, and beam lengths were chosen so a force of 1 N produced by the propeller would be magnified to use the maximum load cell force rating of 2.943N.

MATLAB was used to generate solution tables of suitable beam lengths that satisfied these two conditions. Beam lengths were chosen from the solution tables based on numbers that were easiest to cut from a fabrication standpoint and dimension that fit in a reasonable thrust stand footprint.

### III. Electrical & Transducer Design

The thrust stand's electrical system was designed with heavy consideration of accuracy and versatility. In addition to controlling some peripheral circuitry, the electrical system's primary concern involved measuring the force generated by the thrust of the propeller using a transducer. The transducer used by the thrust stand was a load cell, utilizing a series of strain gages in a Wheatstone bridge circuit configuration. The load cell converted the force into an appropriate electrical signal that could be registered, measured, and recorded using a microcontroller subsystem. All transducer measurements and data acquisition was facilitated by an Arduino UNO microcontroller.

#### A. Signal Amplification & Conditioning

Given the nature of the force under examination and the desired quality of measurement, a load cell was selected as the measuring transducer. In practice, a load cell converts a physical applied force into an electrical signal. Given the relatively small nature of the force under examination, a load cell from a standard 300 gram chemical scale was used. Based on the specification of the chemical scale, the load cell had an uncertainty of  $\pm 0.1g$  and an excitation voltage of approximately 2.5 volts.

In practice, the typical output voltage of a load cell is within the millivolt range, outside the typical range of most ADC ranges. Moreover, signal amplification was desired to increase the amplitude of the signal to a range applicable to a desired ADC range. However, rather than using a single differential operational amplifier (Op-Amp) circuit to amplify the differential voltage at the output terminals of the load cell, a circuit configuration using three op-amps known as an instrumentation amplifier was used. Better input signal impedance can be achieved through the use of an instrumentation amplifier. This signal input impedance is not always present using a single differential op-amp circuit. Therefore, using an instrumentation op-amp circuit can achieve a higher accuracy and precision in the associated measurement.<sup>3</sup>

For ease and simplicity of design, a prepackaged instrumentation amplifier was used for the thrust stand's electrical system. Due to its cost effectiveness and common use and support, the INA125P instrumentation amplifier was used. The INA125P features single precision differential input, a single amplified output, and an amplification gain that can be adjusted using a single resistor between two of the associated pins. Additionally, the INA125P features three selectable precision reference voltages (2.5VDC, 5VDC, and 10VDC). These reference voltages were found to be particularly useful in supplying a reliable and consistent excitation voltage of 2.5 volts to the load cell,

greatly reducing the internal electrical noise of the system, increasing the overall reliability of the measurement.<sup>3</sup>

After initial integration of the electrical system with both the mechanical and software and the initial testing was conducted, consistent periodic noise became a substantial issue. In addition to general transient electrical noise, high periodic signal noise was noticeable throughout the signal range, concentrating around approximately 8Hz and 15Hz. These frequencies were determined to be the load cell responding to the natural resonate oscillation of the mechanical setup and additional vibrations created by the propeller and rubber-band unwinding rapidly.

To combat this noise issue and more accurately represent the desired thrust data, a standard Butterworth low-pass filter was added to the output signal from the instrumentation amplifier. Rather than tailoring the filter's cutoff frequency closer to the unwanted periodic noise, the cutoff frequency of the filter was designed with respect to a lower cutoff frequency of approximately 3Hz. Since the desired thrust signal should demonstrate practically no periodic traits, this lower cutoff frequency was desirable. Moreover, the filter should remove not only the unwanted periodic noise but also some of the transient electrical noise. The schematic diagram of this low-pass filter design is depicted in Figure 2.

To calculate the resistive and capacitive values depicted in Figure 2 associated with approximate desired cutoff frequency, Eq. 2 was used.

$$f_c = \frac{1}{2\pi RC} = \frac{1}{2\pi(4.7k\Omega)(10\mu F)} \approx 3.3863Hz \quad (2)$$

In Eq. 2,  $f_c$  represents the desired cutoff frequency measured in Hertz,  $R$  represents the resistive value of the resistive element in the low-pass filter measured in Ohms, and  $C$  represent the capacitive value of the capacitive element of the low-pass filter measured in Farads. By manipulating the resistive and capacitive values to  $4.7k\Omega$  and  $10\mu F$  respectively, an approximate cutoff frequency of 3.3863Hz was created. At this cutoff frequency the unwanted periodic and transient noise is sufficiently removed from the INA125P's signal.<sup>3</sup>

Integrating both the amplification and filter circuits together created the necessary signal conditioning required to fully utilize the Arduino Uno's standard 5 volt ADC range and create a clean and consistent output signal. For added functionality, three peripheral potentiometers were added to the amplification circuit setup. Acting as low-range-high-precision voltage dividers, two of the potentiometers were connected between the load cell's output terminals and the INA125P's input terminals. The purpose of these two potentiometers were to adjust the differential voltage from the load cell and effectively balance the corresponding Wheatstone bridge. This balancing was necessary to compensate for any initial applied load from the mechanical design and/or any possible preexisting hysteresis in the load cell. The third potentiometer acted as an adjustable gain for the INA125P, allowing the sensitivity of measurement to be adjusted.

Based on the information supplied by the INA125P's datasheet, the gain of the INA125P follows Eq. 3, depicted below.

$$V_{out} = (V_{in}^- - V_{in}^+) * \left(4 + \frac{60k\Omega}{R_G}\right) \quad (3)$$

In Eq. 3,  $V_{out}$  represents the output signal voltage of the INA125P,  $V_{in}^-$  and  $V_{in}^+$  represents the voltage at each input of the INA125P, and  $R_G$  represents the resistance of the external resistor (a potentiometer in this design) between the external gain adjustment terminals of the INA125P. Based on Eq. 3 (and experimentally verified), the maximum resistance of the potentiometer was selected to be  $10k\Omega$ , striking a compromise between a high sensitivity range and an appropriate amplified voltage range, fully unitizing the Uno's ADC range.

Additionally, precautionary decoupling capacitors were added to both the excitation voltage rails of the load cell and the input voltage rails of the INA125P to ensure a stable and consistent power supply. A schematic diagram of the final signal conditioning electrical setup is depicted below in Figure 3.

## B. Electrical Integration:

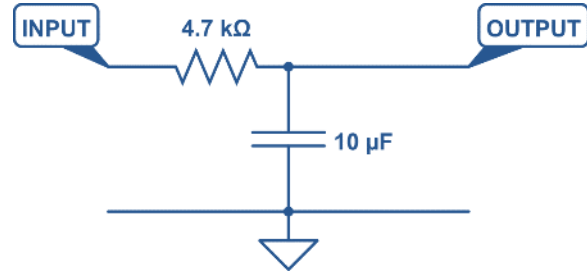
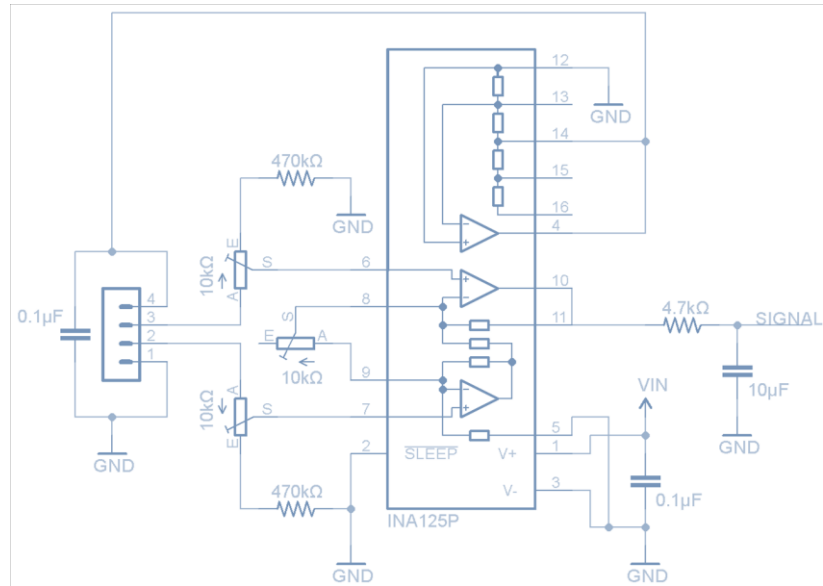


Figure 2 Butterworth low-pass circuit schematic.

All signal conditioning and peripheral circuitry was interfaced with an Arduino UNO microcontroller, creating the completed data acquisition system. Arduino is a popular open-source platform (both in hardware and software) for microcontroller programming. It is intended to function as simple, relatively cost effective, and user friendly electronic prototyping platform. The Arduino platform consists of a wide variety of developmental boards, each catering to certain prototyping demands. Arduino development boards and the Arduino IDE are designed to use Atmel microcontrollers via the Arduino bootloader. By automatically configuring the hardware resources, the Arduino bootloader greatly simplifies user programming in the IDE.



**Figure 3 Load cell amplification & filter circuit.**

The Arduino development board used in this project was the Arduino UNO. Utilizing Atmel's ATmega328P microcontroller, the Arduino UNO consists of several interfacing pins. These pins include 14 digital input/output (I/O) pins (6 of which can function as PWM outputs), 6 analog input pins, and several varieties of power interfacing pins (5V, 3.3V, GND). The UNO also features a USB communications port used for interfacing with an external computer, an external power input socket, a reset button, and an ICSP header used for re-loading the Arduino bootloader to the ATmega328P chip and for more involved programming.

A particularly useful feature of the Arduino UNO is its ability to easily interface with prepackaged circuits known as Shields. Utilizing the socket header pin design of the Arduino UNO, shields can stack directly on top of the UNO using male header pins. Shields allow easy integration of peripheral electrical circuits, expanding the capabilities of the UNO. In this project, an Arduino UNO prototyping shield was used to integrate the aforementioned circuits with the UNO.

By soldering the signal conditioning and peripheral circuitry onto an Arduino Uno prototyping shield, straight forward integration with the Arduino Uno can be achieved, leading to a more streamlined and clean design. Additionally, by integrating the circuitry in this manner, much of the transient electrical noise is reduced and the process of the mechanical integration of the overall electrical system becomes less complicated.

An external 9 volt wall-adapter power supply powered the Arduino Uno and all additional circuitry, connected to the Arduino Uno's power supply input socket. While most of the project circuitry was either powered from the Uno's 5 volt power rail or the INA125P's reference voltages, the INA125P was powered using the raw 9 volt supply, supplemented by the Uno's "Vin" power pin. This was done to ensure appropriate signal amplification, avoiding unwanted amplifier saturation. Additionally, a 1000µF decoupling capacitor was attached to the raw 9 volt power supply rail to ensure a reliable and clean supply was maintained for the INA125P, avoiding variance in the signal amplification.

#### IV. Software Design

The software for operating the thrust stand was developed with the goals of usability and reliability. Software development was divided into two components: the data acquisition system and the GUI. The data acquisition system consisted of embedded system software for controlling the UNO developed in Atmel Studio. The data acquisition system was responsible for taking measurements using the UNO and transmitting measurements to the computer. Commands are sent to the data acquisition system from the computer to initiate and terminate the measurement sequence. To allow the user to easily interact with the data acquisition system, the MATLAB GUI was also developed. The GUI was designed for simple and intuitive use so students could quickly learn how to operate the thrust stand. MATLAB was chosen for the development of the GUI because many students and faculty in the

engineering department have experience developing and debugging software in MATLAB. The GUI presents measurements to the user in an easy-to-understand manner and saves the data in an excel spreadsheet for further analysis.

### A. Graphical User Interface

A graphical user interface was developed in MATLAB for collecting and analyzing thrust data from the DAQ. The GUI plots data in real time as it is collected from the serial port. Using the GUI, students can quickly determine the maximum thrust, average thrust, and impulse generated by a thrust test; this allows multiple groups to perform tests with the thrust stand in a standard class period. An image of the main GUI window is provided in Figure 4.

All user interaction with the thrust stand occurs via the left pane of Figure 4 which is divided into four panels: Status, Calibration, Noise Reduction, and Results. A test is initiated by selecting the appropriate serial port from the drop down in the Status pane and pressing the start button. The connection between the data acquisition system and the computer is established and allowed to stabilize during the initialization phase. The program then enters the zeroing phase. MATLAB determines the zero reading of the force sensor by computing the average of a 5 second no load reading from the load cell. A 5 second countdown is provided on the status indicator during the zeroing sequence. After the zeroing sequence, a servo releases the rubber band propeller and the data acquisition process begins. Data is plotted in real time on the right side of the GUI during the test. Once a test run is complete, max force, average force, and impulse are provided in the results section. The user can adjust the bounds to determine the interval over which the results are calculated.

Due to the small magnitude of the forces measured by the thrust stand, thrust measurements are susceptible to external vibrations and noise. Fortunately, most of these interference components are periodic in nature, and the thrust stand tends to oscillate at a natural resonant frequency between 7 and 9 Hz. Noise can be removed from the thrust stand data using the built in noise reduction utility. Checking the reduce noise checkbox passes the data through an FFT; all frequency components above a user specified cutoff frequency are removed. The updated plot is displayed in the right pane. The noise reduction utility is non-destructive; unchecking the checkbox restores the original plot of the data. A cutoff frequency between 3 and 5 Hz provides clean thrust curves without significantly distorting thrust data. A discussion of the routines used for noise reduction is provided in the signal analysis section. Finally, raw and noise-reduced data are exported as an Excel spreadsheet by pressing the save button. The data are given an automatic date and time stamp and exported to the working directory from which the MATLAB program is running.

### B. Data Acquisition System

Early versions of the data acquisition system software were written in the Arduino IDE. However, the Arduino IDE is designed for hobbyist use and introductory programming, not scientific data acquisition. The group ran into a challenge obtaining equispaced data from the Arduino IDE at the desired sampling rates. This is because many of the Arduino library functions, such as the serial port functions, are designed for compatibility across multiple microchips; the overhead associated with this compatibility reduces the efficiency of the Arduino IDE. After researching the capabilities of the ATmega328P, the microchip used on the UNO, the group decided to program the chip directly. Final software for the data acquisition system was written in C using Atmel Studio 6.1. The ATmega328P on the Arduino UNO can be directly programmed over the ISCP header provided on the board.

The primary motivation behind programming the ATmega328P directly was the desire to achieve a high sampling rate with equispaced data. The ATmega328P ADC has the capability to be triggered automatically by an onboard timer counter module. This allows equispaced measurements to be guaranteed on a hardware level. The functionality is depicted graphically in Figure 5.

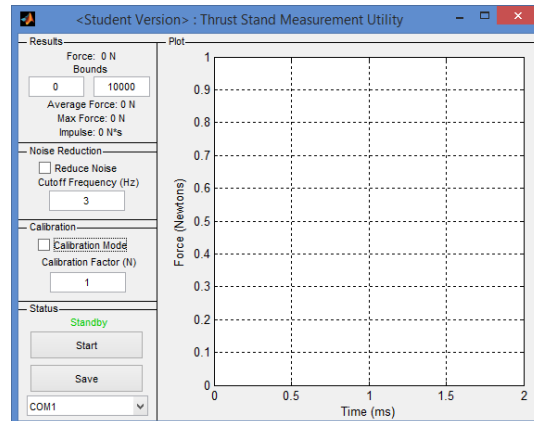


**Figure 4 GUI main window.** Thrust curves are plotted in the right pane of the window. Statistics and user controls are provided in the left pane.

In Figure 5, the Trigger source signal represents a waveform generated by a trigger mechanism. When this trigger source is high, the ADC clock is initialized and an ADC conversion begins. After the conversion is complete, data is output via the ADCH and ADCL registers and an interrupt is triggered via ADIF. When an interrupt is triggered, the data acquisition program reads data out of the ADCH and ADCL registers and prints the data along with an index counter over the serial port.

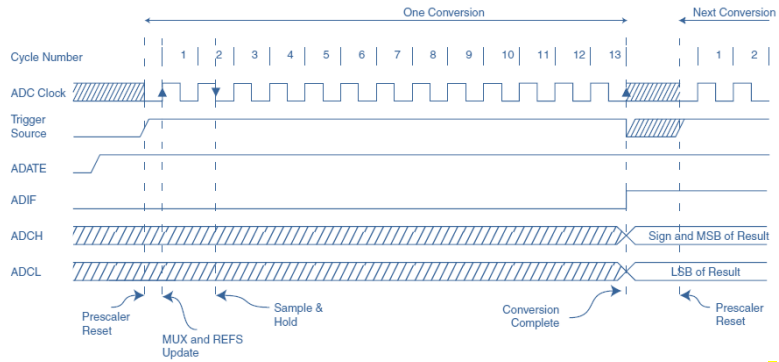


**Figure 5 ATmega328P Auto-Triggered ADC Conversion Sequence<sup>1</sup>**

The trigger mechanism used was an onboard Timer/Counter module integrated into the 328p. The Timer/Counter can be configured to use the 328p system clock in conjunction with a clock prescaler to count to a specified threshold value. Once the threshold value is reached, the Timer/Counter module resets and counting begins again. For the data acquisition software, the Timer/Counter module was configured to reset 1000 times a second; this corresponds to an ADC sampling frequency of 1 kHz. The Timer/Counter frequency is controlled by choosing the Timer/Counter overflow value. An appropriate Timer/Counter overflow value was found using the following equation from the 328p datasheet<sup>1</sup>.

$$f_{timer} = \frac{f_{clock}}{P(1+O)} \quad (4)$$

Where  $f_{clock}$  is the clock frequency in hertz, P is the prescaler value in hertz, O is the overflow value, and  $f_{timer}$  is the timer frequency. Using a timer frequency of 1000 Hz, Eq. 4 can be solved for the overflow value given the system clock and an appropriate prescaler. A prescaler must be chosen that keeps the overflow value within the bit limits of the timer. The Timer/Counter used for triggering the ADC was an 8 bit counter, therefore the maximum overflow value was 255 (starting from 0). A prescaler of 64 provides an appropriate overflow value:

$$O = \frac{f_{clock}}{P * f_{timer}} - 1 = \frac{16000000Hz}{64(1000)} - 1 = 249$$

An overflow value of 249 is below the maximum of 255, therefore, providing the 8 bit Timer/Counter with the overflow value of 249 and prescaler of 64 produces a sampling rate of exactly 1000 Hz.

## V. Performance

### A. Noise Characterization and Signal Analysis

Initial thrust stand tests revealed significant mechanically induced noise in thrust measurements. An early thrust curve produced with the thrust stand is provided in Figure 6. Due to the amplitude and frequency of the noise, it was impossible to characterize the maximum thrust or total impulse. Figure 6 also demonstrates that the noise was mechanically induced since the amplitude of the noise decreases as the rubber band and propeller stop spinning. The team suspected that the noise was caused by the bouncing of the under-constrained rubber band and propeller assembly as the rubber band unwound.

Due to the periodic nature of the noise, Fourier analysis was an appropriate tool for characterizing the noise and identifying the cause of the interference. Data from the thrust stand were transformed to the frequency domain using MATLAB's fast Fourier transform function. The MATLAB FFT function makes use of the Cooley-Turkey algorithm for converting data to the frequency domain<sup>2</sup>. The absolute value was taken of the resulting transform and imaginary components of the FFT were discarded. The resulting distributions were plotted for analysis.

The FFT of the Figure 6 thrust data is provided in Figure 7. A strong peak is present at approximately 8 Hz, and smaller peaks exist at 15Hz and higher frequencies. Similar peaks of approximately 8 Hz were identified in all thrust measurements. It was suspected that the 8Hz peak was the natural resonant frequency of the thrust stand. To test the theory, the moment arm of the thrust stand was tapped with a metal object to create resonance while recording data.

The FFT of the resultant data revealed a peak at 8Hz, supporting the team's theory that the natural resonant frequency of the thrust stand was approximately 8Hz. Regardless of the cause of the 8Hz peak, the information from the FFT characterized the noise source adequately so the team could develop noise reduction techniques.

The team took a two-sided approach to noise reduction by approaching the problem from an electrical and software perspective. The electrical circuit was modified with passive filtering to reduce noise before digital conversion on the Arduino Uno. A passive low pass Butterworth filter with a cutoff frequency of 3.386Hz was installed in the circuit between the instrumentation amplifier and the Arduino UNO. The LPF was an appropriate solution for noise reduction because the thrust generated by the propulsion system that translates to forward motion is non-periodic. This is seen visually in Figure 7; the amplitude of frequency components below 1 Hz is much larger than all events above 1 Hz with the exception of the 8 Hz noise signature. The LPF reduced the magnitude of frequency components above 3.386 Hz while keeping the low frequency thrust measurements intact.

The LPF significantly reduced the magnitude of the noise in thrust measurements. Figure 8 is an FFT of thrust measurements with the LPF installed. The magnitude of the 8Hz peak is significantly reduced in relation to the low frequency components, and noise above 30Hz is almost completely removed. The thrust curve for the Figure 8 FFT is provided in Figure 9; it is a significant improvement over the thrust curve provided in Figure 6.

A software routine based on the MATLAB FFT function was also developed to allow the user to further reduce noise after data collection. The routine first converted the thrust measurements into the frequency domain. The amplitude of frequency components above a user specified cutoff frequency were then replaced with zeroes, effectively removing high frequency components of the thrust data. The MATLAB inverse FFT function was then used to reconstruct a new thrust curve based on the modified frequency domain. The result was a software low pass filter with a hard cutoff frequency. Because the cutoff frequency is user controlled, the student can decide how strong of a noise reduction is appropriate for a given thrust test. The noise reduced thrust data is stored under a different array name so the student can revert back to the original thrust data or change the cutoff frequency at any time.

A sample noise reduced thrust curve with a cutoff frequency of 3 Hz is shown in Figure 10. As compared to Figure 9, almost all noise is removed from the thrust curve. However, aberrations that are a product of the noise

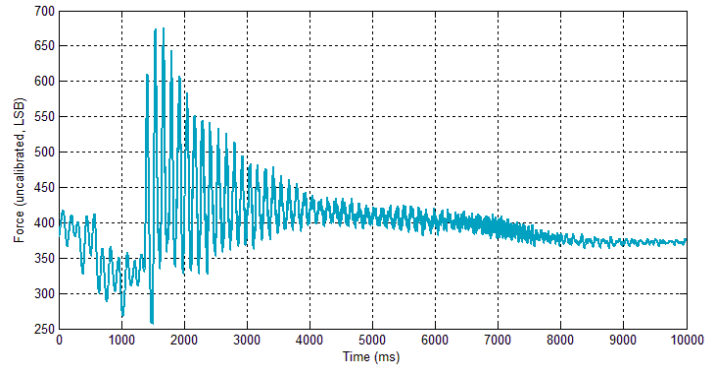


**Figure 6 Unfiltered, thrust measurements plotted as a function of time.** *It is impossible to characterize the maximum thrust or total impulse due to the significant mechanical interferences.*

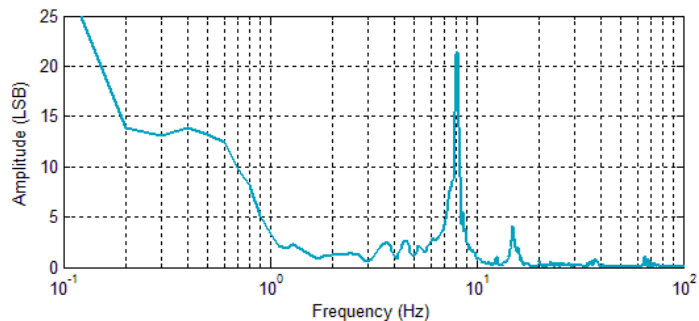


**Figure 7 Unfiltered thrust measurements plotted in frequency domain.** *Note the strong peak at 8Hz. The 8Hz interference is present in all thrust measurements.*

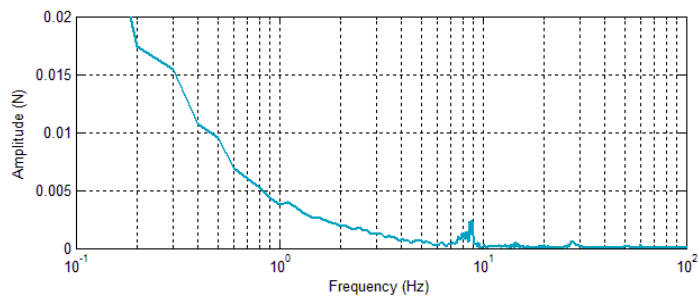


**Figure 8 Thrust measurements plotted in frequency domain with inclusion of a passive low pass Butterworth filter.** *Note the strong reduction in the relative magnitude of the 8Hz peak compared to low frequency components.*

reduction algorithm are visible at the beginning and end of the thrust curve. The flat lines visible before and after the thrust test in Figure 9 are converted to sinusoidal waves in Figure 10. These aberrations occur due to the hard cutoff frequency associated with the software filter. Rapid jerks and high speed events, such as the initial jump to peak thrust, are not properly represented in the noise reduced thrust curve because these events include high frequency components that are removed by the software filter. However, these high frequency events are of little interest for determining the peak thrust or total impulse, and the elimination of most noise is a fair compromise for small distortions in the thrust data at the beginning and end of the thrust test.

The authors recognize that MATLAB also includes built in software filters. The use of a software Butterworth filter would reduce the sinusoidal aberrations seen in the current version of the software filter by softening the cutoff slope. The lab group was unaware of the existence of these functions and how to use them during initial development of the GUI. If the MATLAB data analysis routine were rewritten, the group would probably decide to implement one of these algorithms. However, the routine utilizing the MATLAB FFT function performs adequately given the shape of the thrust curves produced by the thrust stand.

### A. Sample Results

Numerous test measurements were completed with the thrust stand to develop a laboratory procedure for students and to characterize the performance of the thrust stand. A few sample results are provided to demonstrate the capabilities of the thrust stand. Table 1 provides maximum thrust, average thrust, and impulse for three unique rubber band windings; plots of the three thrust tests are provided in Figure 11. The maximum thrust, average thrust, and impulse are distinct for each test case in Table 1; this indicates that the thrust stand produces measurements that are accurate enough to discern between different rubber band winding configurations. Though not demonstrated in Table 1 or Figure 11, thrust measurements were also found to be fairly repeatable for the same test setup. All measured parameters varied by a few hundredths of a Newton or Newton-second during repeated tests since initial winding conditions were never exactly the same for each thrust test, and the rubber band gradually wore out over repeated tests. However, the general shapes of the thrust curves for repeated tests were nearly identical.

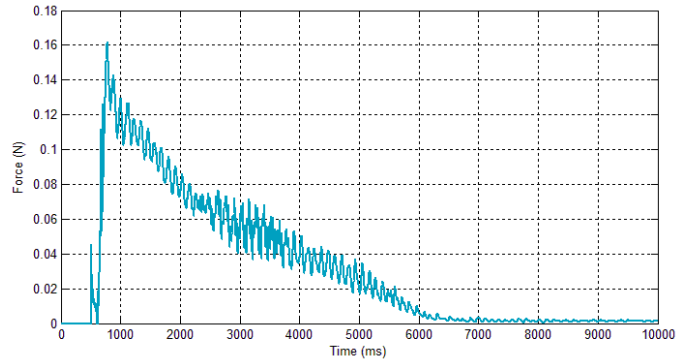


**Figure 9** Sample thrust curve with low pass Butterworth filter installed. Note the significant reduction in noise as compared to Figure 6.

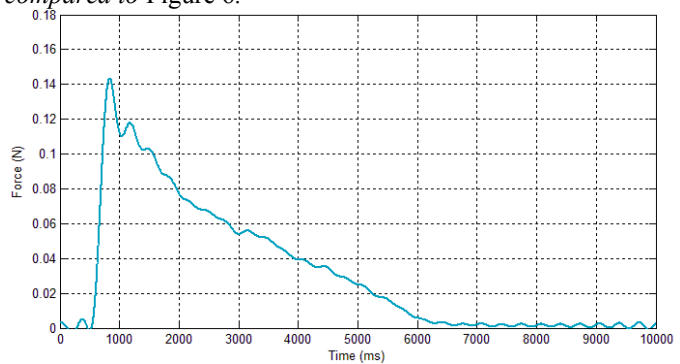


**Figure 10** Sample thrust curve after software noise reduction set at 3Hz. Almost all noise is removed from the curve.

	100 turns, not doubled	50 turns, doubled	150 turns, not doubled
Max Thrust (N)	0.12300	0.33331	0.19374
Average Thrust (N)	0.05799	0.16524	0.05969
Impulse (N*sec)	0.20884	0.23148	0.32533

**Table 1** Sample results for max force, average force, and impulse for three different thrust tests.

Figure 11 demonstrates that increasing the number of turns in the rubber band increases total thrust and impulse, while doubling over the rubber band significantly increases peak thrust but does not necessarily increase total impulse. Students should be able to easily compare how the propeller and rubber band configuration planned for their rubber-band airplane design project affects thrust output. Therefore, the thrust stand fulfills the basic requirements established at the beginning of the project: that students be able to use the thrust stand to better characterize the performance of their rubber band aircraft and use the information to optimize their designs.

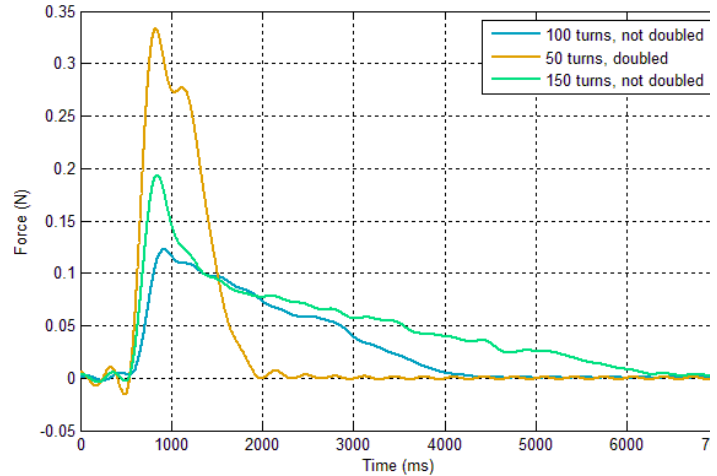


**Figure 11 Comparison of noise-reduced thrust curves for three different winding conditions.**

### B. Measurement Uncertainty Analysis

Propagated uncertainty analysis was carried out by finding the measurement uncertainty in the major components of the DAQ. The uncertainty of the system was then calculated by adding each of the errors using the error propagation formula.

Load cell uncertainty was determined from the manufacturer specifications for the scale from which the load cell was obtained. The scale was listed to have an uncertainty of  $\pm 0.05g$ . The mass uncertainty was converted to a force uncertainty using the acceleration of gravity.

An identical procedure was used to find the uncertainty in the calibration factor. Masses used during the calibration procedure were measured on a scale with an uncertainty of  $\pm 0.05g$ . Therefore, the calibration uncertainty is identical to the load cell measurement uncertainty.

ADC uncertainty was derived from the calibration slope measured during the calibration procedure. The calibration slope defines the linear relationship between force and ADC voltage readings and has units of Newtons per ADC step. Therefore, the ADC uncertainty equals plus or minus half the calibration slope. This value is approximately 0.233 mN.

Precision uncertainty was included to quantify uncertainty due to electrical noise, ambient vibration, and other sources of error not included in the preceding uncertainty terms. Precision uncertainty was estimated by taking a 10 second static reading from the load cell. A 95 percent confidence interval was calculated for the single measurement uncertainty based on the data. A sample calculation for the confidence interval is provided below:

$$u_{precision} = \pm z * S_x \tag{5}$$

$$u_{precision} = 1.9599 * 1.1075ADC = \pm 2.1706ADC$$

The precision uncertainty above has arbitrary units of ADC steps. The precision uncertainty was converted to units of force by multiplying by the calibration factor. The resultant precision uncertainty was 1.01mN. Table 2 provides a summary of the uncertainty components.

The total measurement system uncertainty was calculated from the uncertainties in Table 2 using the error propagation formula. It is assumed that errors in the measurement system add linearly:

$$U_{total} = \sqrt{U_{load\ cell}^2 + U_{calibration}^2 + U_{precision}^2 + U_{precision}^2} \tag{6}$$

$$U_{total} = \sqrt{.491^2mN + .491^2mN + .233^2mN + 1.01^2mN} = \pm 1.25mN \text{ or } \pm 0.00125N$$

The single measurement uncertainty was found to be  $\pm 0.00125N$ .

Load Cell Measurement Uncertainty:	$\pm 0.491 \text{ mN}$
Calibration Uncertainty:	$\pm 0.491 \text{ mN}$
ADC Uncertainty:	$\pm .233 \text{ mN}$
Precision Uncertainty:	$\pm 1.01 \text{ mN}$

**Table 2 Summarized sources of uncertainty**

## VI. Conclusion

The thrust stand and supporting software developed by the team met all requirements established for integration into the undergraduate aerospace engineering curriculum at the University of Alabama in Huntsville. The thrust stand is capable of producing scientific measurements with a level of precision that is acceptable for student use. The software and GUI developed for interfacing with the thrust stand enable student groups to easily perform repeated tests with the thrust stand within limited class time. Noise and interference challenges were successfully mitigated through software and electrical system improvements. Finally, the total cost of the thrust stand was kept within financially acceptable limits for the mechanical and aerospace engineering department.

The team sees the experience gained through the design and construction of the thrust stand as applicable to future potential research projects. The current version of the thrust stand has little potential for significant scientific merit since rubber band propulsion systems are not used within the aerospace field beyond basic demonstrations of powered flight. However, it would not be difficult to scale the current version of the thrust stand design for use with more sophisticated and relevant propulsion systems, such as the brushless motors adapted for use with quad rotors and UAV's. The team is also considering using the thrust stand to study the impact of propeller design on thrust curves. This research project would make use of the University of Alabama in Huntsville's rapid prototyping capabilities to develop a variety of propeller designs for testing with the thrust stand. This research project could be pursued with the current rubber band propulsion system, but could also be explored with propulsion systems based on electric motors to reduce the impact of transient effects on thrust measurements.

## Acknowledgments

The team thanks the University of Alabama in Huntsville Mechanical and Aerospace Engineering Department for their financial support, and the Student Engineering Design and Prototyping Facility for manufacturing support during project development. The team would also like to thank members of the faculty including Dr. Armentrout and Dr. Landrum as well as fellow students who provided valuable suggestions and advice on how to move the project forward and address specific challenges during project development.

## References

<sup>1</sup>Atmel., "Atmel 8-bit Microcontroller with 4/8/16/32Kbytes In-System Programmable Flash," [datasheet], URL: <http://www.atmel.com/Images/doc8161.pdf> [cited 3March 2014].

<sup>2</sup>MATLAB., "R2013b Documentation: fft," [datasheet], URL: <http://www.mathworks.com/help/matlab/ref/fft.html> [cited 3March 2014].

<sup>3</sup>T. G. Beckwith, R. D. Marangoni and J. H. Lienhard, Mechanical Measurements (6th Edition), Pearson Prentice Hall, 2007.